Reversible *intra*molecular hydrogen transfer between cysteine thiyl radicals and glycine and alanine in model peptides: absolute rate constants derived from pulse radiolysis and laser flash photolysis

Thomas Nauser[⊥], **Giulio Casi**[⊥⊥], **Willem H. Koppenol**[⊥], and **Christian Schöneich**[¶,*]

[⊥]*Institute of Inorganic Chemistry, ETH Zürich, 8093 Zürich, Switzerland* [⊥⊥]*Institute of Organic Chemistry, ETH Zürich, 8093 Zürich, Switzerland* [*]*Department of Chemistry and Applied Biosciences, ETH Zürich, 8093 Zürich, Switzerland* [¶]*Department of Pharmaceutical Chemistry, 2095 Constant Avenue, University of Kansas, Lawrence, KS 66047*

Abstract

The *intra*molecular reaction of cysteine thiyl radicals with peptide and protein $^\alpha$C-H bonds represents a potential mechanism for irreversible protein oxidation. Here, we have measured absolute rate constants for these reversible hydrogen transfer reactions by means of pulse radiolysis and laser flash photolysis of model peptides. For N-Ac-CysGly$_6$ and N-Ac-CysGly$_2$AspGly$_3$, Cys thiyl radicals abstract hydrogen atoms from Gly with $k_f = (1.0\text{-}1.1)\times10^5$ s^{-1}, generating carbon-centered radicals, while the reverse reaction proceeds with $k_r = (8.0\text{-}8.9)\times10^5$ s^{-1}. The forward reaction shows a normal kinetic isotope effect of $k_H/k_D = 6.9$, while the reverse reaction shows a significantly higher normal kinetic isotope effect of 17.6, suggesting a contribution of tunneling. For N-Ac-CysAla$_2$AspAla$_3$, cysteine thiyl radicals abstract hydrogen atoms from Ala with $k_f =(0.9\text{-}1.0)\times10^4$ s^{-1}, while the reverse reaction proceeds with $k_r = 1.0\times10^5$ s^{-1}. The order of reactivity, Gly > Ala, is in accord with previous studies on *inter*molecular reactions of thiyl radicals with these amino acids. The fact that $k_f < k_r$ suggests some secondary structure of the model peptides, which prevents the adoption of extended conformations, for which calculations of homolytic bond dissociation energies would have predicted $k_f > k_r$. Despite $k_f < k_r$, model calculations show that *intra*molecular hydrogen abstraction by Cys thiyl radicals can lead to significant oxidation of other amino acids in the presence of physiologic oxygen concentrations.

Keywords

thiol; thiyl radical; hydrogen transfer; glycine; glycyl radical; alanine; alanyl radical; peptide; disulfide; pulse radiolysis; laser flash photolysis

Introduction

The reversible H-transfer between glycine radicals, GlyC$^\bullet$, and cysteine (reaction 1) plays an important role in various enzymatic processes, such as the activation of pyruvate formate lyase (PFL), ribonucleotide reductase (RNR) III, and benzylsuccinate synthase.[1-5]

$$GlyC^{\bullet} + CysSH = Gly + CysS^{\bullet} \tag{1}$$

The extent to which equilibrium 1 is located on either side will depend predominantly on the local environment around the Gly residue.[2] If the $C_{\alpha}^{\bullet}$ radical center of GlyC[•] is part of an ideal planar system, allowing for maximal capto-dative stabilization in a fully extended peptide structure, where $\Phi, \Psi = 180°$, the GlyC[•] radical will be more stable than CysS[•]. Under such conditions, theoretical data predict that the C_{α}-H bond dissociation energy of Gly, $BDE(C_{\alpha}-H) = 330\text{-}350$ kJ/mol,[2,6] is lower than the S-H bond dissociation energy of Cys, $BDE(S-H) = 341\text{-}370$ kJ/mol.[2,7] However, the incorporation of Gly into stretches of secondary structure can significantly raise the $BDE(C_{\alpha}-H)$,[8] for example to $BDE(C_{\alpha}-H) = 361$ kJ/mol within a β-sheet and $BDE(C_{\alpha}-H) = 402$ kJ/mol within an α-helix. In PFL, the forward reaction of equilibrium 1 (between Gly[734] and Cys[419]) triggers the enzymatic turnover, while the reverse reaction of equilibrium 1 restores the resting state of the enzyme.[4,5] It appears that moving equilibrium 1 towards one or the other side requires conformational changes around Gly[734] which would render the GlyC[•] radical more or less reactive towards the adjacent Cys residues, i.e. fine-tune the C_{α}-H BDE.[2] An analogous mechanism should operate in RNR III: here, DFT calculations of electron spin resonance (ESR) hyperfine properties of the GlyC[•] radical were able to confirm a planar configuration of GlyC[•] in *E. coli* RNR but a non-planar structure in bacteriophage T4 anaerobic RNR, essentially demonstrating two conformations of GlyC[•] in two related enzymes.[9]

Despite a large number of theoretical calculations, experimental data on the rate constants of equilibrium 1 and the intramolecular reaction of Cys thiyl radicals with amino acids, in general, are scarce. Kinetic NMR measurements at 37°C and acidic pH provided rate constants for the bimolecular reaction of cysteamine thiyl radicals with glycine anhydride (3.2×10^5 M^{-1}s^{-1})[10] (which favorably agrees with a theoretically predicted rate constant, 1.5×10^5 M^{-1}s^{-1}, for the reaction of glycine anhydride with CH$_3$S[•][11]), N-acetylglycine amide (6.4×10^4 M^{-1}s^{-1}),[10] glycyl amide (0.7×10^4 M^{-1}s^{-1}),[12] and Gly (0.3×10^4 M^{-1}s^{-1}).[12] Pulse radiolysis was employed to measure the rate constant for the reaction of Cys thiyl radicals with anionic Gly (3.2×10^5 M^{-1}s^{-1}).[13] An *intra*molecular H-transfer reaction of Cys thiyl radicals was quantified for the tripeptide glutathione under conditions where the N-terminal amino group is deprotonated;[14,15] here, the H-transfer from the C_{α}-H bond of γ-Glu yields a capto-datively well stabilized radical. However, absolute rate constants for *intra*molecular H-transfer reactions between Cys thiyl radicals and α-amino acids within a peptide skeleton (i.e. not N-terminal amino acids) are unknown. The present paper will

$$\underset{|}{-}\overset{|}{C_{\alpha}}{}^{\bullet} + CysSH \rightleftharpoons \underset{|}{-}\overset{|}{C_{\alpha}}-H + CysS^{\bullet} \tag{2}$$
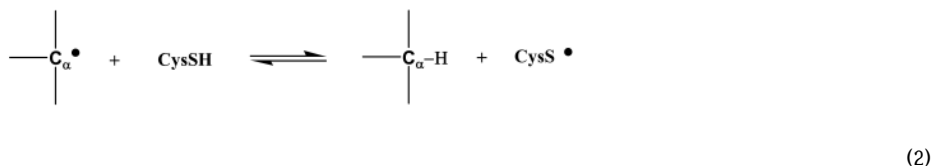
provide kinetic data for such *intra*molecular H-transfer reaction represented by the general equilibrium 2 for the peptides N-Ac-CysGly$_6$, N-Ac-CysGly$_2$AspGly$_3$, and N-Ac-CysAla$_2$AspAla$_3$. The peptide, N-AcCysGly$_6$, containing six Gly residues, was selected for the following reasons: (i) For an efficient H-transfer to occur, the peptide should be sufficiently flexible to allow for the appropriate geometry. Statistically, this should be easier when multiple Gly residues are present within the peptide, though mass spectrometric data[16] with linear heptapeptides suggest that H-transfer to CysS[•] occurs predominantly with Gly residues in position i+1 and i-1. (ii) The solution conformation of Gly$_6$ within a peptide has been

experimentally described[17] as significantly more elongated than the ideal α-helix but more compact than β-strand and polyglycine II, i.e. the Gly_6 moiety in N-Ac-CysGly$_6$ is expected to possess secondary structure. This observation somehow contradicts the results of gas phase calculations, which predict that poly-Gly should prefer an α-helical conformation[18,19] but is consistent with FTIR and Raman spectroscopy data on the even smaller peptide congener Gly_3, which clearly demonstrate Φ and Ψ values significantly different from 180°.[20] In other words, in the Gly_6 sequence of N-Ac-CysGly$_6$ we cannot expect GlyC$^\bullet$ to adopt a fully planar conformation, and, consequently, we expect GlyC$^\bullet$ to be rather reactive. This expectation is consistent with our experimental results described in this paper. The peptide N-Ac-CysAla$_2$AspAla$_3$ was selected to study the reversible H-transfer between Cys thiyl radicals and Ala, where the amino acid Asp was introduced into the middle of the polyAla sequence in order to prevent hydrophobic association (based on our previous bimolecular rate constants, we do not expect a significant reaction of CysS$^\bullet$ with Asp[10]). For direct comparison of Gly and Ala, we also evaluated the peptide sequence N-Ac-CysGly$_2$AspGly$_3$.

Experimental

Materials

N-Ac-CysGly$_6$ was synthesized in two independent batches using Fmoc chemistry by G.Casi (Laboratorium für Organische Chemie, ETH Zürich, Switzerland) and by the Biochemical Research Service Laboratory (BRSL) at the University of Kansas. N-Ac-CysAla$_2$AspAla$_3$ and N-Ac-CysGly$_2$AspGly$_3$ were synthesized by the BRSL at The University of Kansas. All peptides were purified by reversed-phase HPLC and their purity assessed by mass spectrometry. N-Ac-Cys, N-Ac-Cys-OMe, (CysGly)$_2$ (disulfide), Gly$_6$ and N-Ac-Ala-NH$_2$ (all >99% grade) were obtained from Bachem (Bubendorf, Switzerland). 2-Mercaptopropionylglycine (>97%) and N-Ac-Gly-NH$_2$ were purchased from Fluka AG (Buchs SG, Switzerland) and ABCR GmbH (Karlsruhe, Germany), respectively. Water (H_2O) was taken from a Millipore MilliQ system. Deuterium oxide of 99.8% quality was provided by E.I.R. (Switzerland).

Pulse radiolysis

A Febetron 705 (L-3 Communications, San Leandro, CA) 2 MeV accelerator at the ETH Zürich delivered pulses of 5-50 Gy dose. As light source a 75 W Xe arc lamp was used. The detection system consisted of an Acton SP300i monochromator (Roper Scientific, Ottobrunn, Germany) and a Hamamatsu R928 photomultiplier (Hamamatsu Photonics, Solothurn, Switzerland). The signal was digitized and recorded on a Yokogawa DL7100 digital storage oscilloscope (NBN Elektronik AG, Uitikon, Switzerland) and subsequently transferred to a PC. Samples were gas saturated in Schlenk-tubes which were repeatedly evacuated to 10 mbar and refilled with the desired gas. Afterwards, they were taken out via needle into gas tight syringes (Hamilton SampleLock, 10 ml) and introduced into the Hellma 1cm quartz measurement cell (Mülhausen, Germany) through a flow system. The transfer of the samples (transfer to the syringe and from there to the cell) reintroduced some oxygen back into the solutions. The concentration was determined independently to be smaller than 6 μM.

Laser Flash Photolysis

Laser flash photolysis (LFP) experiments were carried out with an Applied Photophysics LKS 50 instument (Leatherhead, UK), equipped with a Quantel Brilliant B Nd:YAG Laser (Les Ulis, France) of which the 4th harmonic was used. The oscilloscope of the original instrument (LKS 50) has been replaced by a LeCroy Waverunner 64Xi oscilloscope (Geneva, Switzerland). The measurement cell consisted of a 1 cm Hellma fluorescence cell, equipped with a Youngs type valve to ensure maximal air-tightness. The cuvettes were several times

evacuated to 10 mbar (i.e. boiling) and refilled with the desired gas. They were virtually oxygen free. Unless stated otherwise, samples were irradiated only once.

Errors

All experiments reported here have been reproduced at least five times. Often, additional experiments have been carried out with different detection wavelength, pH or concentration (data not shown or referred to). The rate constants derived from pulse radiolysis are *reproducible within 10%* between experiments. Controls with a different sample handling and detection system using our laser flash photolysis setup lead essentially to the same rate data as derived by pulse radiolysis. In flash photolysis we can enforce larger uncertainties if we change assumptions (*vide infra*). Then the rate constants derived by computer simulation vary up to 20%. The dose determination in pulse radiolysis (initial concentration of radicals) has an error lower than 5%.

If we consider, that the rate data we took from the literature may carry an error of 10% each, we estimate the absolute error on our rate constant below a factor of 2 and the one of the equilibrium constants below 20%

## Results

1. Peptides

Pulse radiolysis

<u>Radiation-induced chemical processes in water:</u> The pulse irradiation of water leads to the formation of protons, hydrated electrons (e_{aq}^-), $^\bullet$H, and hydroxyl radicals ($^\bullet$OH), where hydrated electrons can be converted into $HO^\bullet$ through reaction with N_2O ($k = 9.1 \times 10^9$ $M^{-1}s^{-1}$, $[N_2O]_{sat} \approx 2 \times 10^{-2}$ M).[21] We note that in acidic solution, hydrated electrons also react with protons to yield $H^\bullet$ ($k = 2.3 \times 10^{10}$ $M^{-1}s^{-1}$[22]), i.e. the relative yields of $H^\bullet$ and $HO^\bullet$ will depend on the pH. For N_2O-saturated solutions, the effective radiation chemical yield of $^\bullet$OH converting a given substrate into substrate-derived radicals can be calculated on the basis of formula I given by Schuler et al.,[23] where G refers to the number of species generated/reacted per 100 eV absorbed energy (G = 1.0 corresponds to 0.1036 μM generated/reacted species per 1 J absorbed energy; G^{N2O} refers to G in N_2O-saturated solution).

$$G^{N_2O}(OH^\bullet) = 5.2 + 3.0 \frac{[k_s[S]/(4.7 \times 10^8)]^{1/2}}{1 + [k_s[S]/(4.7 \times 10^8)]^{1/2}}$$

(I)

<u>Radical yields:</u> *N-Ac-CysGly$_6$:* The pulse irradiation of N_2O-saturated aqueous solutions containing $(2-6) \times 10^{-4}$ M N-Ac-CysGly$_6$ and 1×10^{-2} M KH_2PO_4 (pH 4.2) at room temperature leads to the expected transient optical absorptions with $\lambda_{max} = 260$ nm and $\lambda_{max} \approx 330$ nm. [24] Figure 1A displays an absorbance-vs-time trace recorded for 2×10^{-4} M N-Ac-CysGly$_6$ at 260 nm (applied dose = 18 Gy) (the solid line represents a kinetic simulation, which will be discussed separately below). By comparison to published spectra,[24,25] this absorbance is caused by the formation of two radical species, the carbon-centered radical GlyC$^\bullet$, generated through hydrogen abstraction from Gly, and the thiyl radical CysS$^\bullet$, generated through hydrogen abstraction from the sulfhydryl group of Cys (*vide infra*). The absorbance at 260 nm reaches a maximum of 0.011 absorption units (AU[§]) at ca. 5 μs after the pulse. The rate constant for the reaction of $HO^\bullet$ radicals with the Gly$_6$ moiety in N-Ac-CysGly$_6$ (reaction 3; n = position


[§]Absorption units are dimensionless

of GlyC$^{\bullet}$ in the Gly$_6$ moiety; a = n-1; b = 5-a) is taken as k$_3$ = 8×10^8 M^{-1}s^{-1} by analogy to published values for a series of Gly peptides at acidic to neutral pH,[22] and confirmed by our own kinetic simulations of the experimental data (*vide infra*).

$$HO^{\bullet}+N-AcCysGly_6 \rightarrow H_2O+N-Ac-Cys-Gly_a-{}^n(GlyC^{\bullet})Gly_b \tag{3}$$
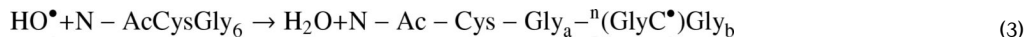
Our kinetic simulation (*vide infra*) yields k$_4$ = 1×10^{10} M^{-1}s^{-1} for the reaction of HO$^{\bullet}$ radicals with the Cys moiety in N-Ac-CysGly$_6$ (reaction 4), similar to the published rate constant for the reaction of HO$^{\bullet}$ with Cys.[22]
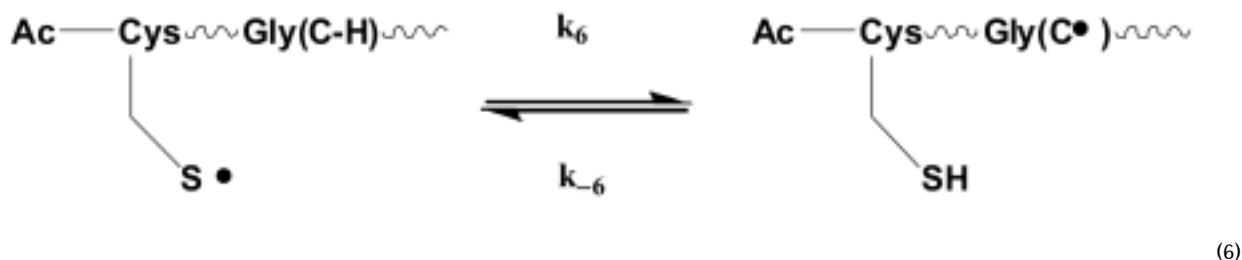
$$HO^{\bullet}+N-Ac-(CysSH)Gly_6 \rightarrow H_2O+N-Ac-(CysS^{\bullet})Gly_6 \tag{4}$$

Taking k(HO$^{\bullet}$+CH$_3$CONH$_2$) = 1.9×10^8 M^{-1}s^{-1} as a representative rate constant for the potential reaction of HO$^{\bullet}$ radicals with the N-acetyl group,[22] we calculate that in N-Ac-CysGly$_6$ ca. 90% of the HO$^{\bullet}$ radicals are expected to react with the Cys moiety. The H$^{\bullet}$ atoms will exclusively react with the Cys moiety in N-Ac-CysGly$_6$, where k$_5$ = 2×10^9 M^{-1}s^{-1} based on our simulations (*vide infra*), which corresponds to the published rate constant for the reaction of H$^{\bullet}$ atoms with Cys, i.e. 1.8×10^9 M^{-1}s^{-1}.[22]

$$H^{\bullet}+N-Ac-(CysSH)Gly_6 \rightarrow H_2+N-Ac-(CysS^{\bullet})Gly_6 \tag{5}$$
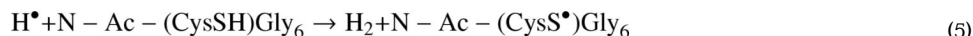
The H$^{\bullet}$ atoms will not react with the Gly moiety of N-Ac-CysGly$_6$ (cf., for the reaction of H$^{\bullet}$ with N-Ac-Gly, k = 3.5×10^6 M^{-1}s^{-1} [22]). Hence, equation I predicts that the total yield of hydroxyl radicals available for reaction with N-Ac-CysGly$_6$ amounts to G = 5.4, of which 91% react with the Cys residue. In addition, H$^{\bullet}$ atoms formed with an initial yield of G(H$^{\bullet}$) = 0.6 will react with the Cys residue so that the overall amount of primary water radicals reacting with the Cys moiety in 2×10^{-4} N-Ac-CysGly$_6$ amounts to 0.91 G$_{HO^{\bullet}}$ + G$_{H^{\bullet}}$ = 5.5. At an applied dose of 18 Gy, and an absorbance coefficient for CysS$^{\bullet}$ at 260 nm of ε$_{260,CysS^{\bullet}}$ ≈ 73 M^{-1}cm^{-1} (*vide infra*), we expect that CysS$^{\bullet}$ radicals would contribute maximally 7.5×10^{-4} AU to the experimentally measured absorbance immediately after the pulse. Initially, 8% of the primary HO$^{\bullet}$ radicals react with the Gly moiety in N-Ac-CysGly$_6$ to give GlyC$^{\bullet}$, responsible for 6.8×10^{-3} AU (based on an absorbance coefficient for GlyC$^{\bullet}$ of ε$_{260}$ = 8,410 M^{-1}cm^{-1}, *vide infra*). Therefore, our experimentally measured maximal absorbance yields of 11×10^{-3} AU at 5 µs after the pulse is significantly higher than expected from the combined initial yields of GlyC$^{\bullet}$ and CysS$^{\bullet}$, clearly demonstrating the formation of additional GlyC$^{\bullet}$ radicals over the experimental time period. Importantly, the absorbance growth over 5 µs after the pulse occurs with t$_{1/2}$ ≈ 0.8 µs, i.e. significantly slower as expected based on k$_4$ = 1×10^{10} M^{-1}s^{-1}, indicating the formation of GlyC$^{\bullet}$ through (i) a slower process following the initial attack of HO$^{\bullet}$ on Cys or (ii) reaction 5 followed by the reaction of CysS$^{\bullet}$ with Gly. The latter becomes even more obvious when the concentration of N-Ac-CysGly$_6$ is increased to 6×10^{-4} M under otherwise similar experimental conditions (Figure 1B). Here, the slow growth of the 260 nm absorbance from 9.5×10^{-3} AU to a maximal yield of ca. 13×10^{-3} AU (at 5 µs after the pulse; Δ = 3.5×10^{-3} AU) following the initial rise occurs with t$_{1/2}$ = 0.7 µs, i.e. comparable to that observed with 2×10^{-4} M N-Ac-CysGly$_6$. This independence on peptide concentration is an important fact suggesting that the slow process is an *intra*molecular reaction. Evidence against the involvement of primary water radicals in the slow process comes from two additional features: first, HO$^{\bullet}$ radicals would react with 6×10^{-4} M N-Ac-CysGly$_6$ with t$_{1/2}$ = 0.1 µs, i.e. significantly faster than the observed slow process. Second, the maximal absorbance increase generated by

the reaction of H$^\bullet$ atoms with the Cys moiety of N-Ac-CysGly$_6$ (reaction 5) would be 8×10^{-5} AU, i.e. only about 2.3% of the observed increase by 3.5×10^{-3} AU.

Hence, these data suggest that the absorbance increase through the slow process is indeed an *intra*molecular process such as the reversible interconversion between CysS$^\bullet$ and GlyC$^\bullet$ (equilibrium 6).

$$\text{Ac—Cys}\sim\sim\text{Gly(C-H)}\sim\sim \quad \xrightleftharpoons[k_{-6}]{k_6} \quad \text{Ac—Cys}\sim\sim\text{Gly(C}^\bullet)\sim\sim$$

$$\begin{array}{cc} | & | \\ \text{S}^\bullet & \text{SH} \end{array}$$

(6)

Reference experiments with Gly$_6$: The pulse irradiation (15 Gy) of 7.2×10^{-4} M Gly$_6$ in N$_2$O-saturated aqueous solution, pH 1.7, leads to the absorption-vs.-time trace displayed in Figure 1c. Here, GlyC$^\bullet$ radicals are exclusively generated through reaction 7 (a = n-1; b = 5-a).

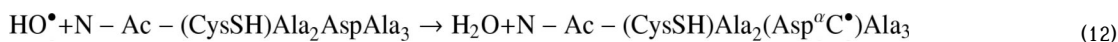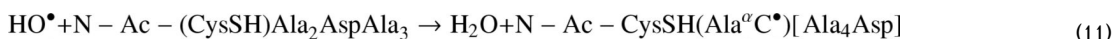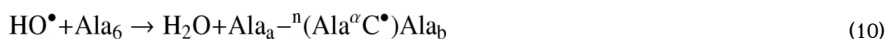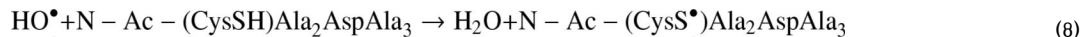$$HO^\bullet + Gly_6 \rightarrow H_2O + Gly_a^n GlyC^\bullet Gly_b$$

(7)

Within 5 μs after the pulse, the absorbance yield reaches a maximum of 0.052 AU. before it decays slowly. A complete spectrum of Gly$_a^n$GlyC$^\bullet$Gly$_b$ is shown in Figure 2A, from where we derive $\varepsilon_{260,GlyC\bullet} = 8{,}410$ M^{-1}cm^{-1} and $\varepsilon_{330,GlyC\bullet} = 2{,}690$ M^{-1}cm^{-1}. Nearly identical values have been obtained for the GlyC$^\bullet$ radical from N-Ac-Gly-NH$_2$[#]. In general, these values are slightly lower than the previously published absorption coefficient (e.g., $\varepsilon_{263} = 12{,}900$ M^{-1}cm^{-1} [24]). However, we note that the previous absorption coefficients for GlyC$^\bullet$ derived from Gly anhydride[25] were also later corrected to lower numbers by others.[26]

Reference experiments with N-Ac-Cys-methyl ester disulfide: The absorption coefficients of CysS$^\bullet$ were independently determined through pulse radiolysis. Figure 2B shows the optical spectra obtained after pulse irradiation of (i) 2×10^{-4} M N-acetylcysteinemethylester disulfide, (N-Ac-Cys-OMe)$_2$ in Ar-saturated aqueous solution, pH 1, containing 90 mM 2,2 dimethylpropanol (tert-butanol, ^{t}BuOH), and (ii) 90 mM ^{t}BuOH in Ar-saturated aqueous solution, pH 1. Under these experimental conditions, all HO$^\bullet$ radicals react with ^{t}BuOH to yield carbon-centered radicals, HO-C(CH$_3$)$_2$CH$_2^\bullet$, while all hydrated electrons convert into H$^\bullet$ atoms, which subsequently reduce the disulfide bond to yield thiol and thiyl radicals of the structure N-Ac-(CysS$^\bullet$)OMe. The difference between both spectra represents the absorption spectrum of N-Ac-(CysS$^\bullet$)OMe, from which we calculate $\varepsilon_{260,N-Ac-(CysS\bullet)OMe} = 73$ M^{-1}cm^{-1} (not corrected for reactant spectra).

N-Ac-CysAla$_2$AspAla$_3$: The pulse irradiation (20.8 Gy) of an N$_2$O-saturated aqueous solution, pH 4, containing 2×10^{-4} M N-Ac-CysAla$_2$AspAla$_3$ yields the absorption vs. time profile displayed in Figure 3 (circles). The 260 nm absorption represents predominantly Ala$^\alpha$C$^\bullet$ radicals, where $\varepsilon_{260,Ala\alpha C\bullet} = 9{,}500$ M^{-1}cm^{-1} (vide infra), and a small fraction of Asp$^\alpha$C$^\bullet$ (ca. 17%), where it can be assumed that $\varepsilon_{260,Ala\alpha C\bullet} \approx \varepsilon_{260,Asp\alpha C\bullet}$. In these experiments we expect the absorbtion after the reaction of the primary radicals to be higher than in the case of N-Ac-

[#]Nauser, T.; Gebicki, J., unpublished results.

Cys-Gly$_6$ because the rate constant for the reaction of the hydroxyl radical with Ala and Asp is higher than with Gly. Therefore we have initially a higher fraction of carbon centered radicals that are formed, based on $k_8 = 1 \times 10^{10}$ M^{-1}s^{-1} (vide infra), $k_9 = 2 \times 10^9$ M^{-1}s^{-1} (vide infra), $k_{10} = 1.7 \times 10^9$ M^{-1}s^{-1} [22] $= (0.83\ k_{11} + 0.17\ k_{12})$ (a = n-1; b = 5-a), and k(HO$^\bullet$+N-acetyl group) $= 1.9 \times 10^8$ M^{-1}s^{-1} [22].

$$HO^\bullet + N - Ac - (CysSH)Ala_2AspAla_3 \rightarrow H_2O + N - Ac - (CysS^\bullet)Ala_2AspAla_3 \tag{8}$$

$$H^\bullet + N - Ac - (CysSH)Ala_2AspAla_3 \rightarrow H_2 + N - Ac - (CysS^\bullet)Ala_2AspAla_3 \tag{9}$$

$$HO^\bullet + Ala_6 \rightarrow H_2O + Ala_a-{}^n(Ala^\alpha C^\bullet)Ala_b \tag{10}$$

$$HO^\bullet + N - Ac - (CysSH)Ala_2AspAla_3 \rightarrow H_2O + N - Ac - CysSH(Ala^\alpha C^\bullet)[\,Ala_4Asp] \tag{11}$$

$$HO^\bullet + N - Ac - (CysSH)Ala_2AspAla_3 \rightarrow H_2O + N - Ac - (CysSH)Ala_2(Asp^\alpha C^\bullet)Ala_3 \tag{12}$$

With radiation yields of G($^\bullet$OH)=5.3 and G($^\bullet$H) = 0.6 we calculate Gε(AlaC$^\bullet$)=0.855 $\times$ 10^{-3}AU/Gy and Gε(CysS$^\bullet$)=0.038 $\times$ 10^{-3} AU/Gy. Therefore, with a dose of 20.8 Gy we predict an initial absorption of 18.6 $\times$ 10^{-3} AU in accordance with the experimentally measured 18.2 $\times 10^{-3}$ AU. Based on the rate constants, we can calculate also an initial product ratio of [AlaC$^\bullet$]/[CysS$^\bullet$] = 0.15.

Importantly, the $^\alpha$C$^\bullet$ radicals generated by secondary reactions will exclusively be Ala$^\alpha$C$^\bullet$ because our earlier experiments on the bimolecular reaction of thiyl radicals with amino acids have shown that thiyl radicals react significantly faster with Ala as compared to Asp.[10] Hence, reaction 13 is quasi irreversible, and any further hydrogen transfer to thiyl radicals would originate from Ala.

$$N - Ac - (CysSH)Ala_2(Asp^\alpha C^\bullet)Ala_3 \rightarrow N - Ac - (CysS^\bullet)Ala_2AspAla_3 \tag{13}$$
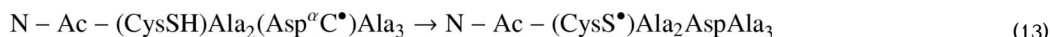
Therefore, ultimately the equilibrium for radicals of N-Ac-CysAla$_2$AspAla$_3$ is best represented by reaction 14, analogous to equilibrium 6 for N-Ac-CysGly$_6$. Experimentally we find (Figure 3, 5 – 30 μs), that the equilibrium is installed by a process that is changing the absorbance to lower values (k$_{-14}$), i.e. K$_{14}$ < 0.15.
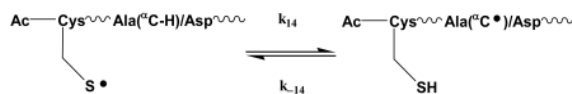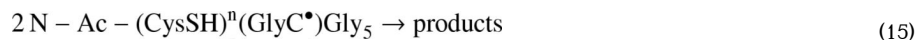

$$\tag{14}$$

Reference experiments with N-Ac-Ala-NH$_2$: A reference spectrum of Ala$^\alpha$C$^\bullet$ was obtained through pulse irradiation of an N$_2$O-saturated aqueous solution, pH 6, of 10 mM N-Ac-Ala-NH$_2$, which is displayed in Figure 2C. Based on the applied radiation chemical dose, we calculate $\varepsilon_{260,Ala\alpha C\bullet}$ = 9,500 M^{-1}cm^{-1} and $\varepsilon_{275,Ala\alpha C\bullet}$ = 8000 M^{-1}cm^{-1}.

<u>**Kinetic analysis:**</u> *N-Ac-CysGly$_6$ and Gly$_6$:* N-Ac-CysGly$_6$ and Gly$_6$ show important differences in the formation of the 260 nm absorbance. In Figure 1C, the 265 nm absorbance after pulse irradiation of Gly$_6$ builds up according to first-order kinetics with $t_{1/2} \approx 1.2$ μs, corresponding to a rate constant for reaction 7 of $k_7 = 8\times10^8$ M^{-1}s^{-1}. For N-Ac-CysGly$_6$, in Figure 1A, the slow build-up of the 260 nm absorbance following the initial rise proceeds according to apparent first-order kinetics with $t_{1/2} = 0.8$ μs. If this process were to represent a pseudo-first order reaction of a primary water radical with 2×10^{-4} μM N-Ac-CysGly$_6$, the bimolecular rate constant for this process would be computed to $k = \ln 2 / t_{1/2}$ [N-Ac-CysGly$_6$] = 4.3×10^9 M^{-1}s^{-1}. Similarly, in Figure 1B the slow build-up proceeds with $t_{1/2} = 0.7$ μs at a concentration of 6×10^{-4} M N-Ac-CysGly$_6$, which would correspond to a bimolecular rate constant $k = 1.4\times10^9$ M^{-1}s^{-1}. If the slow build-up of the 260 nm absorbance were due to the reaction of a primary water radical with N-Ac-CysGly$_6$, we should have obtained similar rate constants (*or* different half-lives) for both peptide concentrations. Therefore, the slow build-up at 260 nm cannot be assigned to any of the reactions of the primary water radicals with N-Ac-CysGly$_6$. These facts, together with the independence of $t_{1/2}$ for the slow build-up on peptide concentrations, are consistent with an *intra*molecular H-transfer from GlyC-H to CysS$^\bullet$ according to the forward reaction of equilibrium 6.

The solid lines in Figures 1A and 1B represent kinetic simulations for two different concentrations of N-Ac-CysGly$_6$, where $k_6 = (1.1\pm0.1)\times10^5$ s^{-1} and $k_{-6} = (8.9\pm0.4)\times10^5$ s^{-1}, i.e. $K_6 = 0.123$ (for a summary of k_6, k_{-6}, and K_6 for all peptides, see Table 1). For these simulations, the initial radical concentrations were determined independently by dosimetry, $\varepsilon_{260,GlyC\bullet}$ = 8,410 M^{-1}cm^{-1} and $\varepsilon_{260,CysS\bullet}$ = 73 M^{-1}cm^{-1} were taken from the experimental spectra displayed in Figures 2A and 2B, $k_3 = 8\times10^8$ M^{-1}s^{-1} was experimentally determined from the build-up of the 260 nm absorbance during the reaction of HO$^\bullet$ radicals with Gly$_6$ (reaction 7; Figure 1C) and $k_{15} = (2.0\pm0.5)\times10^8$ M^{-1}s^{-1} was determined from the bimolecular recombination of Gly$_a$^{n}GlyC$^\bullet$Gly$_b$, generated in reaction 7 (Figure 1C). The rate constants $k_4 = 1\times10^{10}$ M^{-1}s^{-1} and $k_5 = 2\times10^9$ M^{-1}s^{-1} are by analogy to the published rate constants for the reactions of OH$^\bullet$ and H$^\bullet$ with Cys,[22] and $k_{16} = 9\times10^8$ M^{-1}s^{-1} was approximated from the known recombination rate constant of small molecular mass thiyl radicals in aqueous solution,[28] taking into account the slightly larger size of our peptides. A value of $k_{17} = 5\times10^8$ M^{-1}s^{-1} was taken as the mean value between rate constants k_{15} and k_{16}.

$$2\,N-Ac-(CysSH)^n(GlyC^\bullet)Gly_5 \rightarrow products \tag{15}$$

$$2\,N-Ac-(CysS^\bullet)Gly_6 \rightarrow products \tag{16}$$

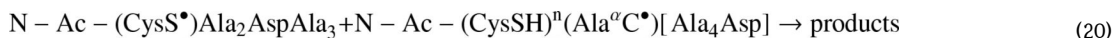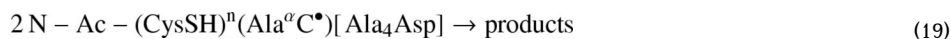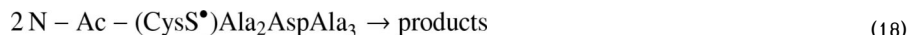$$N-Ac-(CysS^\bullet)Gly_6 + N-Ac-(CysSH)^n(GlyC^\bullet)Gly_5 \rightarrow products \tag{17}$$

Importantly, the same data set was used to simulate the kinetics for our control experiment with Gly$_6$, shown in Figure 1C, except for two modifications reflecting the absence of Cys in this peptide: (1) k_4, k_6, k_{-6}, k_{16} and k_{17} were defined as zero, as those reactions are not possible

during the pulse irradiation of Gly_6; (2) a rate constant $k = 5 \times 10^9$ $M^{-1}s^{-1}$ for the reaction of $H^\bullet$ atoms with $Gly_a{}^n GlyC^\bullet Gly_b$ was assumed.

N-Ac-CysAla₂AspAla₃: As $k_{11} \approx 2 k_3$, [22] initially the fraction of carbon centered radicals is about double that of the case with N-Ac-CysGly$_6$. If there were similar ($K_6 \approx K_{14}$) or lower equilibrium values we would expect the equilibrium to be installed starting with an excess of carbon centered radicals. Indeed, in Figure 3, we see this reflected in the decrease of absorbance in the time range $5 - 30$ μs. The solid line in Figure 3 represents a simulation for 2×10^{-4} M N-Ac-CysAla₂AspAla₃, where $k_{14} = 9.2 \times 10^3$ s^{-1} and $k_{-14} = 1.0 \times 10^5$ s^{-1}, i.e. $K_{14} = 0.092$ (Table 1). The initial radical concentrations were determined by dosimetry, and $\varepsilon_{260,Ala\alpha C\bullet}$ ($\approx \varepsilon_{260,Asp\alpha C\bullet}$) $= 9,500$ $M^{-1}cm^{-1}$ and $\varepsilon_{260,CysS\bullet} = 73$ $M^{-1}cm^{-1}$ were taken from the experimental spectra displayed in Figures 2B and 2C. The other parameters for the simulation were as follows (where [Ala₄Asp] represents the molecular composition of the sequence of the peptide, which does not contain the radical site): $k_8 = 9 \times 10^9$ $M^{-1}s^{-1}$ and $k_9 = 2 \times 10^9$ $M^{-1}s^{-1}$ (approximated from the reactions of $HO^\bullet$ and $H^\bullet$ with Cys[22]), $k_{11} = (k_{12}) = 1.7 \times 10^9$ $M^{-1}s^{-1}$ (by comparison to k_{10}[22]), $k_{18} = 8 \times 10^8$ $M^{-1}s^{-1}$ was approximated from the known recombination rate constant of small molecular mass thiyl radicals in aqueous solution,[28] taking into account the slightly larger size of our peptides, $k_{19} = 2 \times 10^8$ $M^{-1}s^{-1}$ by analogy to k_{15} (vide supra), and a value of $k_{20} = 4 \times 10^8$ $M^{-1}s^{-1}$ was taken as the mean value between rate constants k_{18} and k_{19}.

$$2\,N - Ac - (CysS^\bullet)Ala_2AspAla_3 \rightarrow products \tag{18}$$

$$2\,N - Ac - (CysSH)^n(Ala^\alpha C^\bullet)[\,Ala_4Asp] \rightarrow products \tag{19}$$

$$N - Ac - (CysS^\bullet)Ala_2AspAla_3 + N - Ac - (CysSH)^n(Ala^\alpha C^\bullet)[\,Ala_4Asp] \rightarrow products \tag{20}$$

The two dashed lines in Figure 3 were included in order to demonstrate the sensitivity of the kinetic simulation for the value of k_{-14}. Strong deviations from the experimental data are apparent when values of 8×10^5 s^{-1} and 2×10^4 s^{-1} are used for k_{-14}.

Laser flash photolysis—The double photon ionization of water represents a convenient complementary method to generate primary water radicals ($HO^\bullet$, $H^\bullet$, e^-_{aq}).[29,30] Generally, our 5 ns pulses of 266 nm light (ca. 100mJ), applied to N_2O-saturated water, generated on the order of 3-4 μM hydroxyl radicals, monitored through the oxidation of either Br^- to $Br_2{}^{\bullet-}$ or Cl^- (at pH≤ 3) to $Cl_2{}^{\bullet-}$.

All LFP experiments with Cys-containing peptides were performed under conditions of double photon ionization of water at acidic pH (pH < 5). Under these conditions, there are negligible concentrations of thiolate present, and no direct photoionization of thiolate is observed.[31] All the absorption coefficients were taken from the pulse radiolysis experiments. The kinetic simulations have been carried out under the assumption, that the products and yields of double photon ionization of water is the same in the presence of the peptides as in the presence of Cl^- or Br^-. Therefore, experiments with chloride and bromide were used as a calibration for the yields of primary radicals. This process was chosen in order to minimize the number of variables in the simulation and because we believe it to be physically sensible. We find some unspecified photolysis damage of the peptides upon irradiation with laser light of 266 nm, 2×10^{12} Wm^{-2} power density and 100 mJ energy. At 275 nm, we treat this mathematically as a constant offset (a stepfunction starting with the laser pulse) of the traces in the order of $(3 - 4)$

$\times~10^{-3}$ AU. In terms of chemistry, this corresponds to products of double photon photolysis of the peptides with low product reactivity. Because of this finding, we made no attempt to use our samples for multiple irradiations. At 330 nm detection wavelength, we find no measurable influence of direct photolysis. At this point it should be noted, that the rate constants we derive are (pseudo-)first order and are rather insensitive to the above assumptions.

In addition, in one experiment with cysteinylglycine disulfide, thiyl radicals were generated through the photolytic dissociation of a disulfide bridge (see below).

N-Ac-CysGly$_6$: *Reaction in H$_2$O:* Optical detection at 275 nm after LFP of an N$_2$O-saturated aqueous solution of 6.13×10^{-4} M N-Ac-CysGly$_6$ (data not shown) yields an absorption vs. time profile similar to that shown in Figure 1B, which was fit well over the first 20 microseconds after the laser pulse with a simulation using essentially the same parameters as described above for the pulse radiolysis data. This simulation yields $k_6 = 1.0 \times10^5$ s^{-1} and $k_{-6} = 8.9\times10^5$ s^{-1} ($K_4 = 0.123$) (Table 1), consistent with the pulse radiolysis data.

We then monitored equilibrium 6 at 330 nm, where $\varepsilon_{330,GlyC\bullet} = 2,690$ M^{-1}cm^{-1} and $\varepsilon_{330,CysS\bullet} \approx 100$ M^{-1}cm^{-1} (derived from Figures 2A and 2B). Figure 4a displays the absorption vs. time profile recorded after LFP of 6.13×10^{-4} M N-Ac-CysGly$_6$ in N$_2$O-saturated H$_2$O and, as a control, of a mixture of 6.13×10^{-4} M N-Ac-Cys and 6.13×10^{-4} M N-Ac-Gly-NH$_2$ in N$_2$O-saturated H$_2$O. The latter represents a mixture of the amino acid components of N-Ac-CysGly$_6$, which have no opportunity for *intra*molecular H-transfer. The *inter*molecular rate constant is on the order of 10^5 M^{-1}s^{-1} [10] and the concentrations are below 1 mM. Therefore the *inter*molecular reaction rate is below 10^2 s^{-1}, two to three orders of magnitude slower than our timescale. Because the molar absorptivity for glycyl radicals is virtually the same in Gly$_6$ and N-Ac-Gly-NH$_2$, we get a nice reference of a sample identical to N-Ac-CysGly$_6$, but without *intra*molecular reactions. We do however see some radical recombination reactions (Fig 5). The difference between both traces results in the profile represented by the filled circles, which can be well fitted by first-order kinetics, where $k_{obs,330nm} = k_6 + k_{-6} = 10^6$ s^{-1}. Taking the pulse radiolysis values of $k_6 = 1.1\times10^5$ s^{-1}, we obtain $k_{-6} = k_{obs,300nm} - k_6 = 8.9\times10^5$ s^{-1}, which agrees well with k_{-6} obtained from the pulse radiolysis data.

Kinetic isotope effects: Experiments were then performed in D$_2$O in order to evaluate the kinetic isotope effects of equilibrium 6. The double photon ionization in D$_2$O yields DO$^{\bullet}$, D$^{\bullet}$, and e$^-_{aq}$, where e$^-_{aq}$ reacts further with N$_2$O to give DO$^{\bullet}$ radicals. Figure 4B displays the absorption vs. time profile recorded after LFP of 6.13×10^{-4} M N-Ac-CysGly$_6$ in N$_2$O-saturated D$_2$O and, as a control, of a mixture of 6.13×10^{-4} M N-Ac-Cys and 6.13×10^{-4} M N-Ac-Gly-NH$_2$ in N$_2$O-saturated D$_2$O. Again, a difference trace (represented by the closed circles) is calculated by subtraction of the trace from N-AcCys/N-Ac-Gly-NH$_2$ from that of N-Ac-CysGly$_6$. Figure 4C displays an overlay of the absorbance vs. time profile at 330 nm, recorded for N-Ac-CysGly$_6$ in H$_2$O and D$_2$O. Two important differences between the results in H$_2$O and D$_2$O are apparent. (1) In D$_2$O, the initial absorbance at 330 nm at 500 ns after the laser flash is approximately two-fold higher compared to that in H$_2$O, and this holds also true for the difference traces recorded in H$_2$O and D$_2$O. (2) The difference trace in D$_2$O (Figure 4B) shows a slow decay, measured over ca. 10 μs, in contrast to the difference trace recorded in H$_2$O. Both features can be rationalized. First, the higher initial absorbance at 500 ns after the flash reflects a small increase of the fraction of DO$^{\bullet}$ reacting with the Gly moiety at the expense of the CysSD moiety due to a primary kinetic isotope effect for the reaction of DO$^{\bullet}$ with CysSD (in D$_2$O) vs. HO$^{\bullet}$ with CysSH (in H$_2$O). The absorbance coefficient of GlyC$^{\bullet}$ ($\varepsilon_{330,GlyC\bullet} = 2,690$ M^{-1}cm^{-1}) is significantly higher compared to that of CysS$^{\bullet}$ ($\varepsilon_{330,CysS\bullet} \approx 100$ M^{-1}cm^{-1}), so that the initial absorbance at 330 nm must be higher in D$_2$O than in H$_2$O. This kinetic isotope effect is also reflected in the control experiments in H$_2$O and D$_2$O, where the LFP of the N-Ac-Cys/N-Ac-Gly-NH$_2$ mixture generates a higher initial absorbance in D$_2$O as compared to

H_2O. Second, the slow decay over longer times recorded after LFP of N-Ac-CysGly$_6$ in D_2O suggests a significantly slower adjustment of equilibrium 6 in D_2O compared to H_2O. In H_2O, the reaction of primary radicals with N-Ac-CysGly$_6$ generates an excess of CysS$^{\bullet}$, which then equilibrates under the formation of a higher proportion of GlyC$^{\bullet}$. In contrast, in D_2O the reaction of primary radicals with N-Ac-CysGly$_6$ generates an excess of GlyC$^{\bullet}$, which then equilibrates under formation of a higher proportion of CysS$^{\bullet}$. In D_2O, equilibrium 6 will initially adjust with an overall rate constant $^Dk_{obs,1} = k_6^H + k_{-6}^D$ until all reactive Gly(C-H) bonds are converted into Gly(C-D) when $^Dk_{obs,1}$ changes to $^Dk_{obs,2} = k_6^D + k_{-6}^D$ (our mass spectrometry experiments with linear heptapeptides[16] show that the reaction of CysS$^{\bullet}$ is most efficient with Gly in position i+1 and i-1, i.e. we expect that the most reactive Gly residue in N-Ac-CysGly$_6$ is Gly in position i+1 from Cys). A first-order fit of the difference trace in Figure 4B is shown by the solid line. A more detailed analysis is given in Figure 5, where the absorption vs. time trace in D_2O is fitted (least differences fit) with biexponential kinetics yielding $^Dk_{obs,1} = 1.6 \times 10^5$ s^{-1} and $^Dk_{obs,2} = 6.6 \times 10^4$ s^{-1}. The primary kinetic isotope effects can now be calculated through equations II-V, where in H_2O, $k_{-6}^H = 8.9 \times 10^5$ s^{-1} and $k_6^H = 1.1 \times 10^5$ s^{-1} (Table 1).

$$k_{-6}^D = {}^Dk_{obs,1} - k_6^H = 5 \times 10^4 \, s^{-1} \tag{II}$$

$$k_6^D = {}^Dk_{obs,2} - k_{-6}^D = 1.6 \times 10^4 \, s^{-1} \tag{III}$$

$$k_6^H / k_6^D = 6.9 \tag{IV}$$

$$k_{-6}^H / k_{-6}^D = 17.8 \tag{V}$$

The maximal value of a classic primary isotope effect can be estimated through equation VI,[32] where $\tilde{\nu}_r^H$ represents the wave number of the stretching mode of the reacting X-H bond.
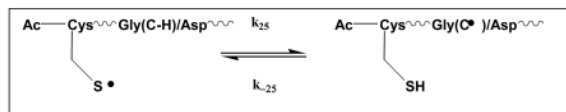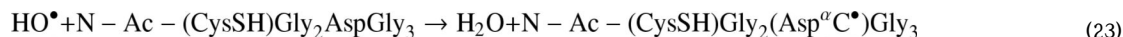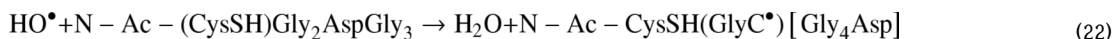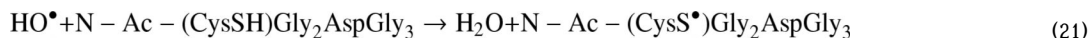
$$\log\left(\frac{k_H}{k_D}\right)_{max} = (3.2 \times 10^{-4})\tilde{\nu}_r^H \tag{VI}$$

For the S-H bond of thiols, $\tilde{\nu}_r^H \approx 2,600$ cm^{-1} [33], so that log $(k_H/k_D)_{max} \approx 0.83$, and $(k_H/k_D)_{max} \approx 6.8$. The latter value agrees well with the experimentally observed $k_6^H/k_6^D = 6.9$. However, the very large kinetic isotope effect $k_{-6}^H/k_{-6}^D = 17.8$ would suggest a contribution of tunneling to the hydrogen transfer process.[34-36]

N-Ac- CysAla$_2$AspAla$_3$: Figure 6 displays an absorption vs. time profile recorded at 275 nm after LFP of 6.13×10^{-4} M N-Ac-CysAla$_2$AspAla$_3$ in N_2O-saturated H_2O. The solid line represents a simulation, where $k_{14} = 1.0 \times 10^4$ s^{-1} and $k_{-14} = 1.0 \times 10^5$ s^{-1}, i.e. $K_{14} = 0.10$ (Table 1). Analogous to the pulse radiolysis experiment, hydroxyl radicals will initially react with Cys, Ala, and Asp (reactions 8, 11 and 12) before final equilibration between CysS$^{\bullet}$ and Ala$^{\alpha}$C$^{\bullet}$ will occur (reactions 13 and 14). The initial radical concentrations were determined

from $\varepsilon_{275,Ala\alpha C\bullet}$ ($\approx \varepsilon_{275,Asp\alpha C\bullet}$) = 8,000 $M^{-1}cm^{-1}$ and $\varepsilon_{275,CysS\bullet}$ = 78 $M^{-1}cm^{-1}$ (vide supra). The other parameters for the simulation were as described for the pulse radiolysis experiments, i.e. $k_8 = 1\times10^{10}$ $M^{-1}s^{-1}$, $k_{11} = k_{12} = 1.7\times10^9$ M^{-1}, $k_{13} = 8.75\times10^3$ s^{-1}, $k_{18} = 8\times10^8$ $M^{-1}s^{-1}$, $k_{19} = 2\times10^8$ $M^{-1}s^{-1}$, and $k_{20} = 4\times10^8$ $M^{-1}s^{-1}$.

N-Ac- CysGly$_2$AspGly$_3$: Analogous to N-Ac-CysAla$_2$AspAla$_3$, the reaction of HO$^\bullet$ radicals with N-Ac- CysGly$_2$AspGly$_3$ will initially target Cys, Gly and Asp (reactions 21-23). Subsequently, Asp$^\alpha$C$^\bullet$ radicals will almost irreversibly react with Cys (reaction -24) and ultimately allow for equilibration between CysS$^\bullet$ and GlyC$^\bullet$ (reaction 25). The latter will occur for the same reason discussed already for N-Ac-CysAla$_2$AspAla$_3$, i.e. the fact that the reaction of thiyl radicals with Gly proceeds significantly faster than the reaction of thiyl radicals with Asp.[10]

$$HO^\bullet + N-Ac-(CysSH)Gly_2AspGly_3 \rightarrow H_2O + N-Ac-(CysS^\bullet)Gly_2AspGly_3 \tag{21}$$

$$HO^\bullet + N-Ac-(CysSH)Gly_2AspGly_3 \rightarrow H_2O + N-Ac-CysSH(GlyC^\bullet)\left[Gly_4Asp\right] \tag{22}$$

$$HO^\bullet + N-Ac-(CysSH)Gly_2AspGly_3 \rightarrow H_2O + N-Ac-(CysSH)Gly_2(Asp^\alpha C^\bullet)Gly_3 \tag{23}$$

$$N-Ac-(CysS^\bullet)Gly_2AspGly_3 \rightarrow N-Ac-(CysSH)Gly_2(Asp^\alpha C^\bullet)Gly_3 \tag{24}$$

$$(25)$$

The LFP of an N$_2$O-saturated aqueous solution of 6.13×10^{-4} M N-Ac-(CysSH)Gly$_2$AspGly$_3$ yielded an absorption vs. time trace at 275 nm (Figure S1; Supplementary Materials), which was well simulated with $k_{25} = 1\times10^5$ s^{-1} and $k_{-25} = 8\times10^5$ s^{-1}, i.e. rate constants expected based on the data presented for N-Ac-CysGly$_6$ (vide supra). Best values for the H$^\bullet$-transfer rate constant in reaction 24 are $k_{24} < 4 \times 10^3$ s^{-1}, $k_{-24} = 4 \times 10^5$ s^{-1} and, consequently, $K_{24} < 0.01$.
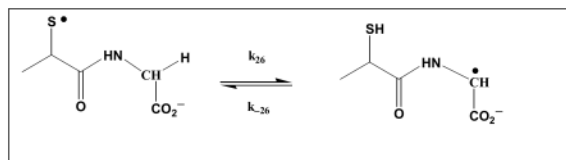
$$(26)$$

2. Reversible H-atom transfer in small model compounds

Experiments with two small models were performed to demonstrate the reversible H-atom transfer with (i) a molecule which essentially only contains a mercaptoalkyl-substituted Gly residue (2-mercaptopropionylglycine) and (ii) an alternative entry into thiyl radicals, i.e. the photolysis of a disulfide bond (cysteinylglycine disulfide).

2-Mercaptopropionylglycine—2-Mercaptopropionylglycine represents a simple model compound for the investigation of reversible intramolecular H-transfer processes between a thiyl radical and Gly. Figure 7 displays the absorption vs. time profiles recorded at 330 nm over 50 μs after the LFP of 6×10^{-4} 2-mercaptopropionylglycine in N_2O-saturated H_2O and D_2O, respectively. As for N-Ac-CysGly$_6$, we observe a higher initial absorbance in D_2O, consistent with a higher relative yield of GlyC$^{\bullet}$ in D_2O compared with H_2O. Importantly, in H_2O there is no further change to the 330 nm absorbance beyond 1 μs after the laser pulse, indicating that any adjustment of equilibrium 26 in H_2O must be significantly faster compared to equilibrium 6 or, more probable, that the primary radical reactions directly create a distribution of thiyl and carbon centered radicals that matches equilibrium 26. On the other hand, for the same experiment in D_2O, we observe a pronounced decay of the 330 nm absorbance over ca. 25 μs. This observation is consistent with an "overproduction" of GlyC$^{\bullet}$ in D_2O, as already described for N-Ac-CysGly$_6$ in D_2O, which subsequently equilibrates with the thiyl radical through equilibrium 26. The decay kinetics in D_2O can be fitted with first-order kinetics, where $^D k_{obs} = 1.38\times10^5$ s^{-1}, again comparable to the value of $^D k_{obs,1} = 1.6\times10^5$ s^{-1} obtained for N-Ac-CysGly$_6$ in D_2O.

Cysteinylglycine disulfide, (CysGly)$_2$—The photolytic cleavage of the cystine disulfide bond yields predominantly thiyl radicals.[37] These thiyl radicals, (CysS$^{\bullet}$)Gly, will equilibrate with GlyC$^{\bullet}$ through equilibrium 27. An important parameter in these experiments is, that the initial radical in both solvents, H_2O and D_2O, is (CysS$^{\bullet}$)Gly(C-H), and that no GlyC$^{\bullet}$ radicals are initially present. This experimental situation is different from the entry into thiyl radicals via the reaction of primary water radicals with Cys-containing peptides and model compounds.

$$(CysS^{\bullet})Gly(C-H)=(CysSH)GlyC^{\bullet} \tag{27}$$

Figure 7 displays an absorbance vs. time trace, recorded at 330 nm, after 266 nm (20 mJ laser energy) photolysis of 1 mM (CysGly)$_2$ in N_2O-saturated H_2O or D_2O containing 1 M ^{t}BuOH, respectively. While the kinetics for absorbance build-up in H_2O and D_2O are of first order, the respective values for k_{obs} are significantly different, $^H k_{obs} = 1.3\times10^6$ s^{-1} and $^D k_{obs} = 6\times10^5$ s^{-1}, respectively. This can be rationalized by the fact that $^H k_{obs} = k_{27} + k_{-27}$ but $^D k_{obs} = k_{27} + k_{29}$ In D_2O, the product of the forward reaction 27, (CysSH)GlyC$^{\bullet}$, undergoes H/D exchange at the mercapto group (reaction 28), yielding (CysSD)GlyC$^{\bullet}$, so that the rate constant for the reverse reaction in D_2O, k_{29}, is smaller than that of the analogous process in H_2O, $k_{-27,H}$.

$$(CysSH)GlyC^{\bullet}+D_2O=(CysSD)GlyC^{\bullet}+HDO \tag{28}$$

$$(CysSD)GlyC^{\bullet}=(CysS^{\bullet})Gly(C-D) \tag{29}$$

In general, the trend of $^H k_{obs} > {}^D k_{obs}$ observed for thiyl radicals from cysteinylglycine is comparable to that observed with all the other investigated peptides and model compounds.

The only difference is the significantly higher numerical values for $^{H}k_{obs}$ and specifically $^{D}k_{obs}$. The signals in these experiments are very low, $(1 - 2) \times 10^{-3}$ AU, and will therefore have a considerable error. We considered these experiments mainly as "proof of concept" but note the good quantitative agreement with the other experiments.

Discussion

The present data provide absolute rate constants for reversible *intra*molecular H-atom transfer between Cys thiyl radicals and the $^{\alpha}$C-H bonds of Gly and Ala in various model peptides. While only $^{\alpha}$C-H bonds are available in Gly, our previous results on bimolecular reactions[12] demonstrate that the $^{\alpha}$C-H group is also the main target for H-atom transfer from Ala. Several important features must be noted. (i) For all peptides under investigation, the rate constant for H-atom abstraction by thiyl radicals (k_6, k_{14}, k_{25}) is lower compared to that for the reverse reaction, H-atom abstraction by the $^{\alpha}$C$^{\bullet}$ radicals from Cys (k_{-6}, k_{-14}, k_{-25}). (ii) The substitution of Gly with Asp at position i+3 relative to Cys has no significant influence on the rate constants for H-atom transfer, evident through comparable values for k_6 and k_{25} and for k_{-6} and k_{-25} for the two peptides N-Ac-CysGly$_6$ and N-Ac-CysGly$_2$AspGly$_3$. This was expected based on our mass spectrometry data with a small linear peptide[16], demonstrating that the residues in position i+1 (and i-1) show the highest reactivity with CysS$^{\bullet}$. (iii) The H-atom transfer reactions show normal primary kinetic isotope effects; however, specifically the large primary kinetic isotope effect of $k_{-6}^{H}/k_{-6}^{D} = 17.8$ suggest that tunneling contributes to the H-atom transfer reaction.

Our earlier kinetic NMR experiments provided rate constants for the bimolecular reaction of cysteamine thiyl radicals with N-Ac-Gly-NH$_2$ and N-Ac-Ala-NH$_2$ of 6.4×10^4 M^{-1}s^{-1} and 1.0×10^4 M^{-1}s^{-1}, respectively,[10] indicating a 6.4-fold faster reaction with the Gly moiety. The *intra*molecular reactions studied in the present work reveal a ca. 12-fold higher reactivity of Gly over Ala (cf. $k_6 = 1.1\times10^5$ s^{-1} and $k_{14} = 9\times10^3$ s^{-1}). Importantly, a similar trend is observed for the reverse reactions, where the average values are $k_{-6} = 8.5\times10^5$ s^{-1} and $k_{-14} = 0.85\times10^4$ s^{-1}, i.e. differ by a factor of 10. Therefore, despite the large differences in the individual rate constants, the average values for the equilibrium constants $K_6 = 0.125$ and $K_{14} = 0.10$ are not too different. The close similarity of these equilibrium constants could be rationalized by the comparable homolytic bond dissociation enthalpies of the $^{\alpha}$C-H bonds of Gly and Ala (BDE = 350 and 345 kJ/mol, respectively), calculated by Rauk et al.[6,7] for fully extended conformations of small model peptides. However, the fact that K_6, $K_{14} < 1.0$ would not be consistent with the absolute numbers, where BDE($^{\alpha}$C-H) = 345 and 350 kJ/mol and BDE(S-H) = 330-370 kJ/mol would predict that K_6, $K_{14} \geq 1.0$. Hence, the low absolute values of K_6 and K_{14} suggest that BDE($^{\alpha}$C-H) > 370 kJ/mol, which would indicate significant secondary structure of the peptides different from a fully extended conformation, and $\Phi, \Psi \neq 180°$. The latter is consistent with spectroscopic data on small Gly and Ala-containing peptides.[17,20]

The biological significance of the measured rate constants will be discussed with the help of Scheme 1, where equilibrium 30 represents the general *intra*molecular H-atom transfer equilibrium between CysS$^{\bullet}$ and $^{\alpha}$C-H.

$$\frac{[^{\alpha}COO^{\bullet}]}{[S^{\bullet}O_2]} = \frac{k_{33}k_{30}(k_{-31}+k_{32})}{k_{32}k_{31}(k_{33}[O_2]+k_{-30})}$$

(VII)

The addition of oxygen to CysS$^{\bullet}$ is reversible,[38] with $k_{31} = 2.2\times10^9$ M^{-1}s^{-1} and $k_{-31} = 6.3\times10^5$ s^{-1}, whereas the addition of oxygen to $^{\alpha}$C$^{\bullet}$ is irreversible ($k_{33} \approx 2\times10^9$ M^{-1}s^{-1}),[39] yielding peroxyl radicals. The latter will serve as precursors for fragmentation pathways as

well as potential chain reactions of protein oxidation.[40,41] The thiylperoxyl radical, CysSOO•, rearranges to the sulfonyl radicals (CysS•O₂) with $k_{32} = 2×10^3$ s⁻¹ (37°C).[38] Assuming steady-state conditions[12], equation VII predicts that at a physiologic oxygen concentration of ca. 30 μM[42], initial CysS• radicals would yield carbon-centered peroxyl radicals from Gly and Ala to an extent of 97% and 94%, respectively, based on the rate constants summarized in Table 1 and, in a first approximation, neglecting any reaction with endogenous glutathione and ascorbate.

$$CysS^\bullet + Asc^- \rightarrow CysS^- + Asc^\bullet \tag{34}$$

If we include the possibility that CysS• radicals react freely with maximally 1 mM ascorbate (Asc⁻; reaction 34; $k_{34} = 6×10^8$ M⁻¹s⁻¹ [43]), ca. 8% of CysS• would convert Gly into carbon-centered peroxyl radicals (reaction 33). Such an efficient reaction with ascorbate is, however, rather unlikely *in vivo* as specifically protein Cys residues will not necessarily be fully accessible to ascorbate. Hence, initially formed protein thiyl radicals will have a pronounced tendency to attack additional amino acids within proteins, leading to precursors for aggregation and fragmentation. This potential role of thiyl radicals has not been given much attention before,[44] as usually thiyl radicals are considered rather stable "sinks" of thiol oxidation processes.

H-atom transfer reactions of thiyl radicals in proteins need also be considered as potential sources for protein degradation in pharmaceutical formulations. Frequently, these formulations contain detergents such as Tween, which accumulate peroxides and react with trace levels of transition metals to yield carbon- and oxygen-centered radicals.[45] The latter will react with protein Cys residues under formation of thiyl radicals, which can then attack the ᵅC-H bonds of additional amino acids resulting in peroxyl radical formation and subsequent fragmentation and aggregation. In this way, the protein Cys residues can function as catalysts for the oxidation of additional amino acid residues, which would normally not be attacked by primary oxidants present in the system. The concept of thiols acting as catalysts for H-transfer reaction between organic radicals and H-donors has been recognized in the field of synthetic organic chemistry (referred to as "polarity reversal catalysis" [46,47]), but may be equally if not more important in the field of protein oxidation relevant to biological conditions of oxidative stress and the biotechnology industry.

Supplementary Material

Refer to Web version on PubMed Central for supplementary material.

Acknowledgements

References

1. Stubbe J, van der Donk WA. Chem Rev 1998;98:705–762. [PubMed: 11848913]

2. Himo F, Siegbahn PEM. Chem Rev 2003;103:2421–2456. [PubMed: 12797836]

3. Himo F, Eriksson LA. J Am Chem Soc 1998;120:11449–11455.

4. Becker A, Fritz-Wolf K, Kabsch W, Knappe J, Schultz S, Wagner AFV. Nat Struct Biol 1999;6:969–975. [PubMed: 10504733]

5. Becker A, Kabsch W. J Biol Chem 2002;277:40036–40042. [PubMed: 12163496]

6. Rauk A, Yu D, Shustov TGV, Block DA, Armstrong DA. Biochemistry 1999;38:9089–9096. [PubMed: 10413483]

7. Rauk A, Yu D, Armstrong DA. J Am Chem Soc 1998;120:8848–8855.

8. Rauk A, Yu D, Armstrong DA. J Am Chem Soc 1997;119:208–217.

9. Himo F, Eriksson LA. J Chem Soc Perkin Trans 2 1998:305–308.

10. Nauser T, Schöneich Ch. J Am Chem Soc 2003;125:2042–2043. [PubMed: 12590520]

11. Reid DL, Armstrong DA, Rauk A, von Sonntag C. Phys Chem Chem Phys 2003;5:3994–3999.

12. Nauser T, Pelling J, Schöneich Ch. Chem Res Toxicol 2004;17:1323–1328. [PubMed: 15487892]

13. Zhao R, Lind J, Merényi G, Eriksen TE. J Am Chem Soc 1994;116:12010–12015.

14. Grierson L, Hildenbrand K, Bothe E. Int J Radiat Biol 1992;62:265–277. [PubMed: 1356129]

15. Zhao R, Lind G, Merényi G, Eriksen TE. J Chem Soc Perkin Trans 2 1997:569–574.

16. Mozziconacci O, Sharov VS, Williams TD, Kerwin B, Schöneich Ch. J Phys Chem B 2008;112:9250–9257. [PubMed: 18611046]

17. Ohnishi S, Kamikubo H, Onitsuka M, Kataoka M, Shortle D. J Am Chem Soc 2006;128:16338–16344. [PubMed: 17165789]

18. Improta R, Barone V, Kudin KN, Scuseria GE. J Chem Phys 2001;114:2541–2549.

19. Improta R, Barone V, Kudin KN, Scuseria GE. J Am Chem Soc 2001;123:3311–3322. [PubMed: 11457067]

20. Schweitzer-Stenner R, Eker F, Huang Q, Griebenow K. J Am Chem Soc 2001;123:9628–9633. [PubMed: 11572684]

21. Von Sonntag, C. The Chemical Basis of Radiation Biology. Taylor & Francis; London: 1987.

22. Buxton GV, Greenstock CL, Helman WP, Ross AB. J Phys Chem Ref Data 1988;17:513–886.

23. Schuler RH, Hartzell AL, Behar B. J Phys Chem 1981;85:192–199.

24. Simic M, Neta P, Hayon E. J Am Chem Soc 1970;92:4763–4768. [PubMed: 5448234]

25. Hayon E, Simic M. J Am Chem Soc 1971;93:6781–6786.

26. Mieden OJ, von Sonntag C. Z Naturforsch 1989;44b:959–974.

27. Hawkins CL, Davies MJ. J Chem Soc Perkin Trans 2 1998:2617–2622.

28. Hoffman MZ, Hayon E. J Am Chem Soc 1972;94:7950–7957.

29. Reuther A, Laubereau A, Nikogosyan DN. J Phys Chem 1996;100:16794–16800.

30. Görner H, Nikogosyan DN. J Photochem Photobiol B: Biology 1997;39:84–89.

31. Tung T, Stone JA. J Phys Chem 1974;78:1130–1133.

32. Schowen RL. Prog Phys Org Chem 1972;9:275–332.

33. Hesse, M.; Meier, H.; Zeeh, B. Spektroskopische Methoden in der Organischen Chemie. Thieme Verlag; Stuttgart: 1979. p. 67

34. Kwart H. Acc Chem Res 1982;15:401–408.

35. Williams F, Sprague ED. Acc Chem Res 1982;15:408–415.

36. Klinman JP. Biochim Biophys Acta 2006;1757:981–987. [PubMed: 16546116]

37. Morine GH, Kuntz RR. Photochem Photobiol 1981;33:1–5.

38. Zhang X, Zhang N, Schuchmann HP, von Sonntag C. J Phys Chem 1994;98:6541–6547.

39. Mieden OJ, Schuchmann MN, von Sonntag C. J Phys Chem 1993;97:3783–3790.

40. Davies MJ. Biochim Biophys Acta 2005;1703:93–109. [PubMed: 15680218]

41. Neuzil J, Gebicki JM, Stocker R. Biochem J 1993;293:601–606. [PubMed: 8352726]

42. Hogan MC. J Appl Physiol 1999;86:720–724. [PubMed: 9931213]

43. Wardman P, von Sonntag C. Methods Enzymol 1995;251:31–45. [PubMed: 7651211]

44. Schöneich, Ch. Chem Res Toxicol 2008;21:1175–1179. [PubMed: 18361510]

45. Harmon PA, Kosuda K, Nelson E, Mowery M, Reed RA. J Pharm Sci 2006;95:2014–2028. [PubMed: 16850394]

46. Roberts BP. Chem Soc Rev 1999;28:25–35.

47. Dang HS, Roberts BP, Tocher DA. J Chem Soc Perkin Trans 1 2001:2452–2461.
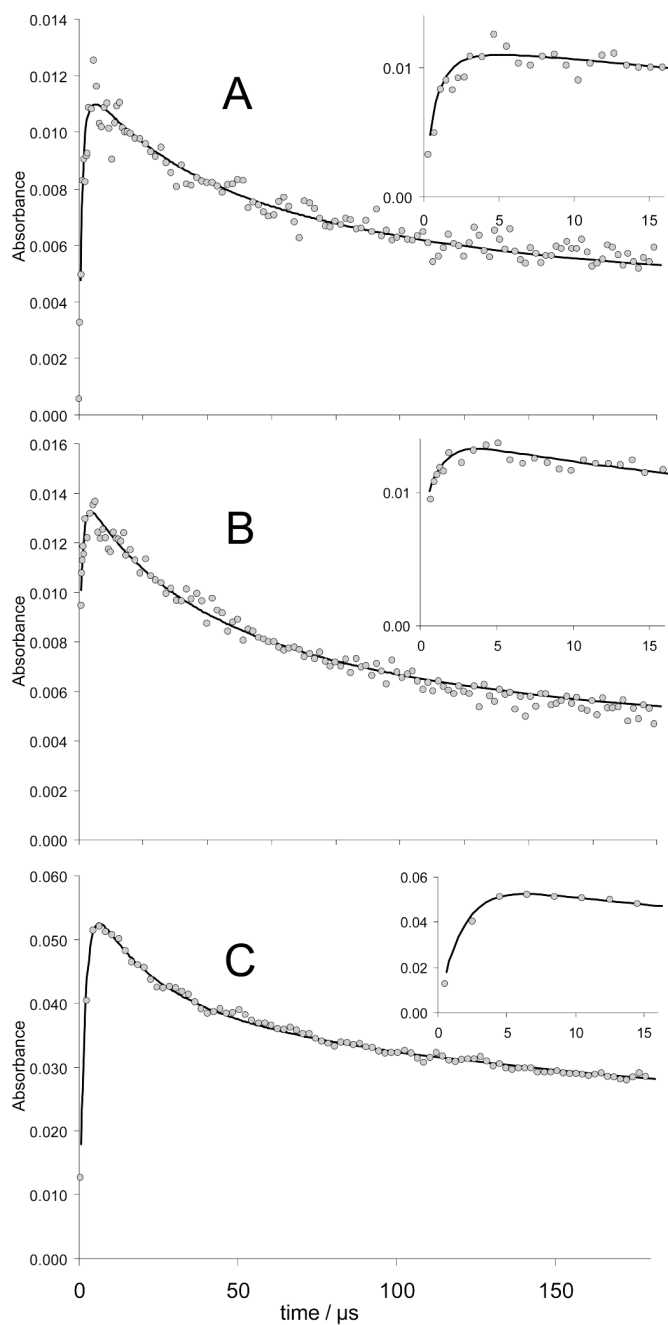
Figure 1.
Pulse radiolysis of N_2O saturated aqueous solutions of 200 μM N-Ac-CysGly$_6$ (Panel A, 18 Gy), 600 μM N-Ac-CysGly$_6$ (Panel B, 20 Gy) and 720 μM Gly$_6$ (Panel C, 15 Gy, control). The experimental traces (dots) are averaged points for specific time periods in order to improve legibility. They are compared with simulations using an identical parameter set. The time-resolved absorption traces in Panels A and B were detected at 260 nm, the one of Panel C at 265 nm. The solutions of N-Ac-CysGly$_6$ contained 10 mM phosphate (pH 4) the one of Gly$_6$ 5 mM H_2SO_4.

Although traces A and B start at different absorption levels, which is due to the reactions of the primary radicals with different concentrations of N-Ac-CysGly$_6$, they reach their maximum at the same time. This indicates a rate determinig step which is 1st order, i.e. *intra*molecular.
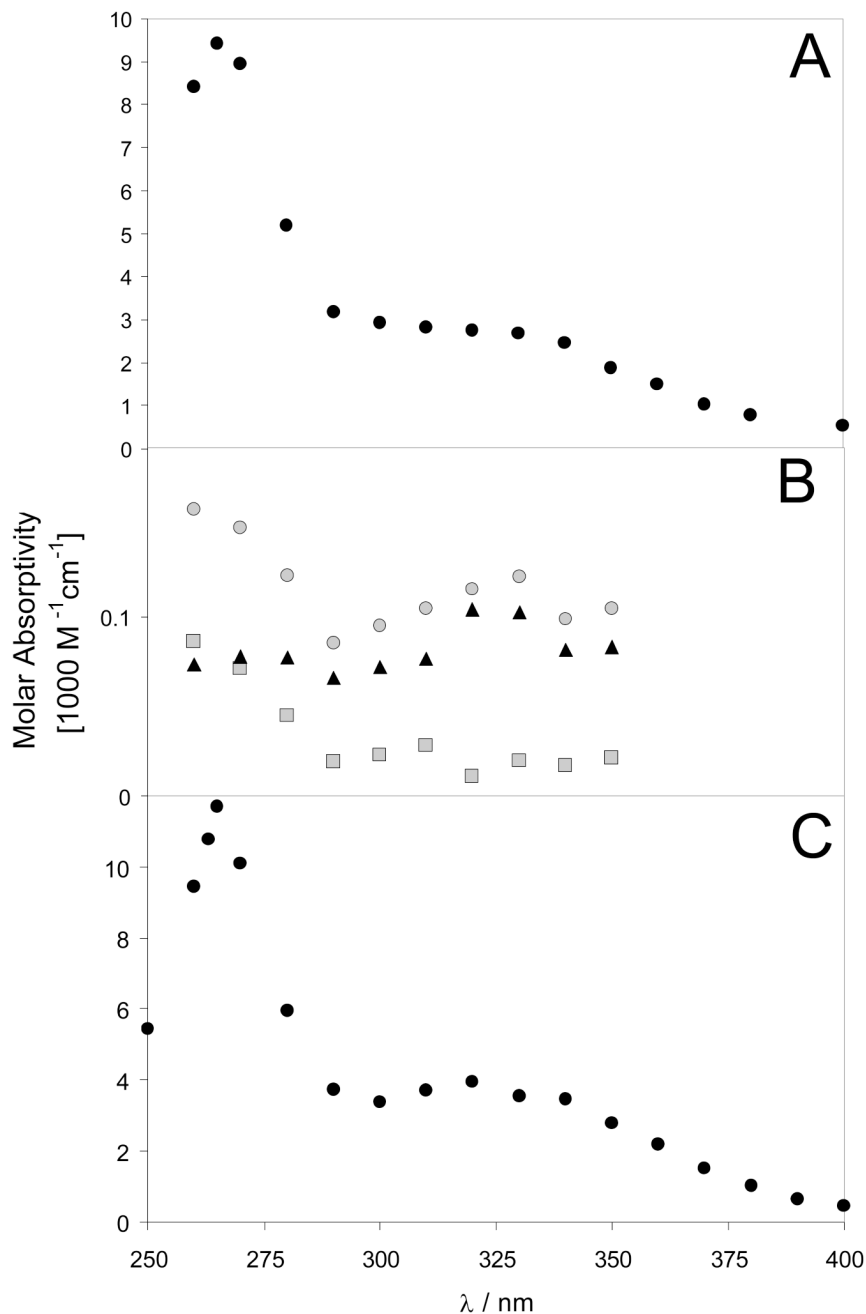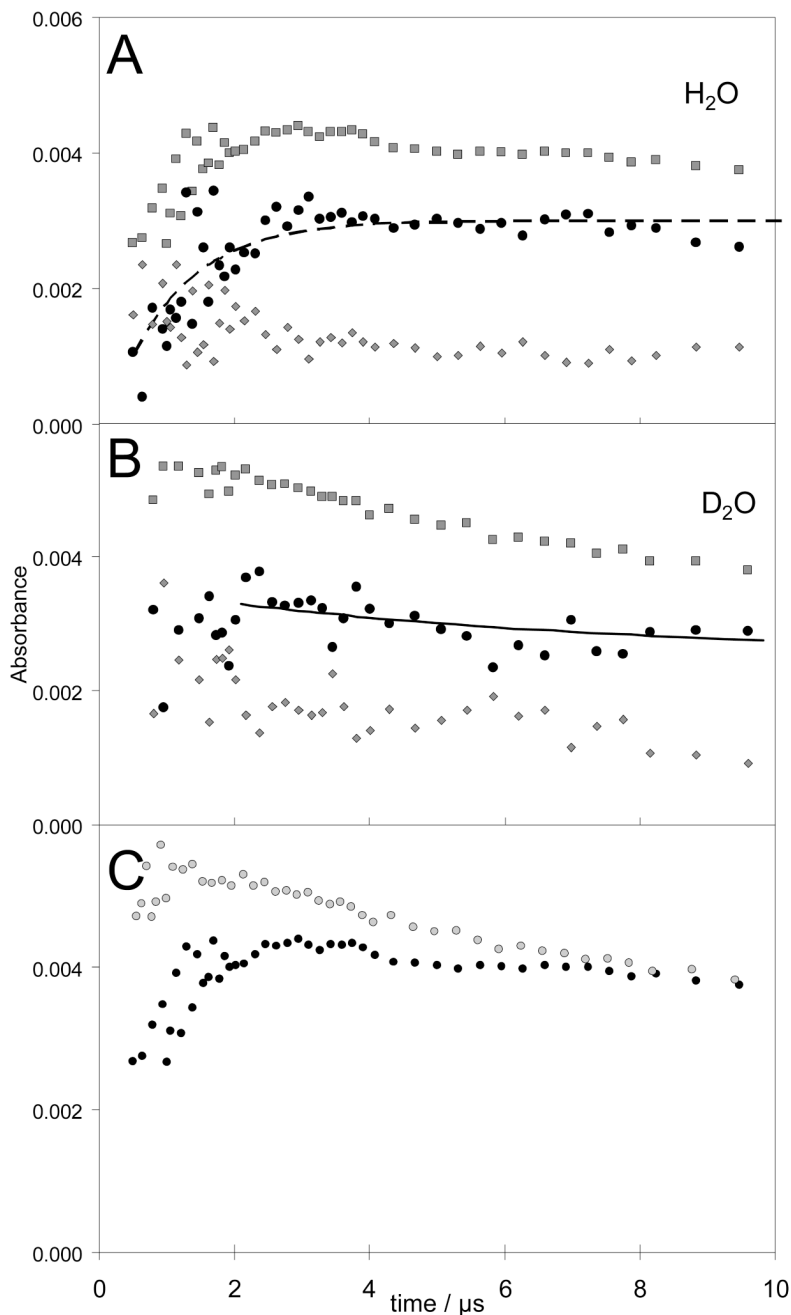
Figure 2.
Spectra of (Gly$_6$)$^\bullet$ (Panel A), N-Ac-CysS$^\bullet$-OMe (Panel B, black triangles) and N-Ac-Ala$^\bullet$-NH$_2$ (Panel C). Experimental conditions were: **Panel A**: 1 mM Gly$_6$, 9 mM H$_2$SO$_4$, N$_2$O-sat., G($^\bullet$OH) = 3.6. **Panel B**: The spectrum of the cysteinyl thiyl radical was derived by a subtraction of a mixed spectrum of thiyl radical and t-butanol radicals (grey circles) and a pure t-butanol radical spectrum (grey squares). The t-butanol spectrum was measured in an argon-saturated solution of 90 mM t-butanol and 90 mM H$_2$SO$_4$. For the mixed spectrum 0.35 mM N-acetylcysteinemethylester (N-Ac-Cys-OMe) was added. G(H$^\bullet$) = 3.1. **Panel C**: 10 mM N-Ac-Ala-NH$_2$, 50 Gy, N$_2$O-sat., 50 Gy
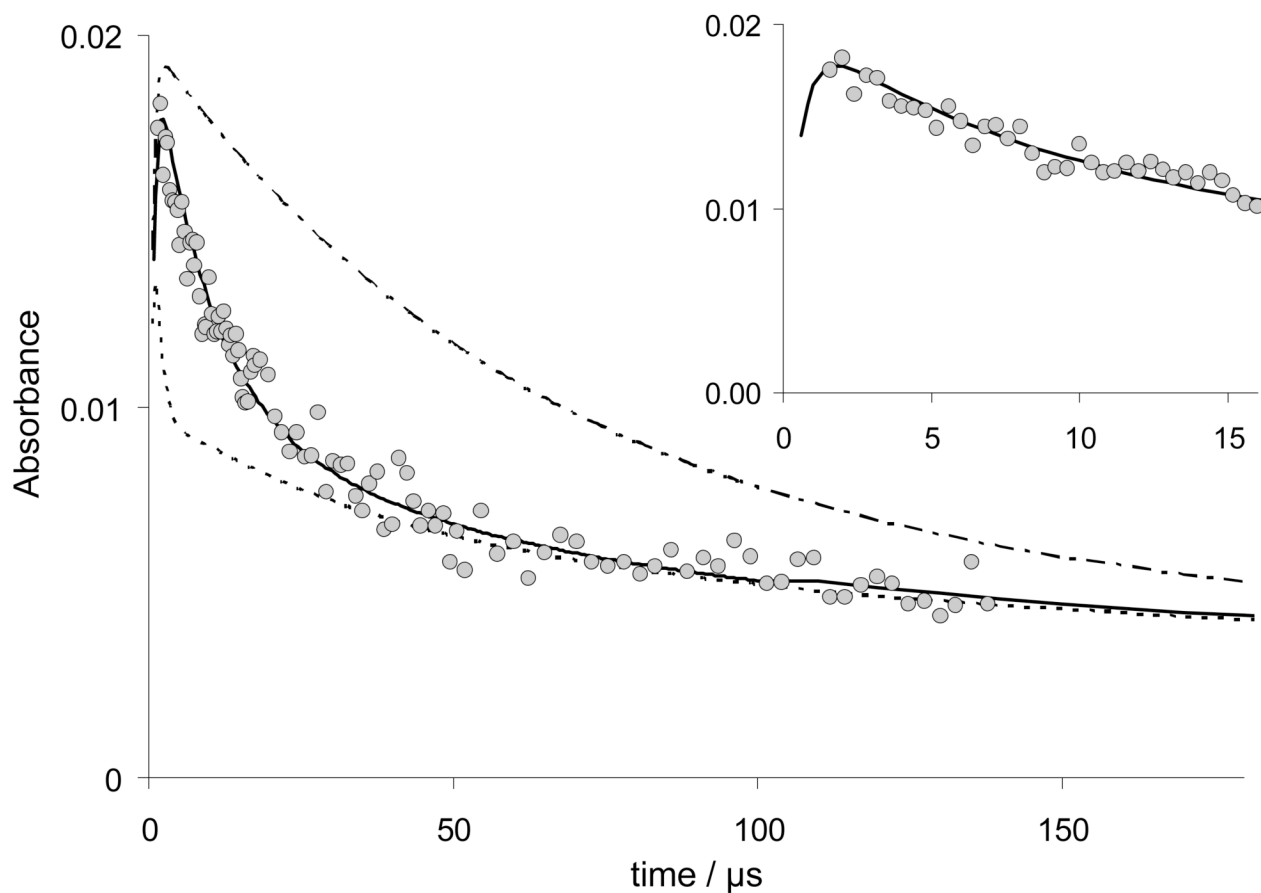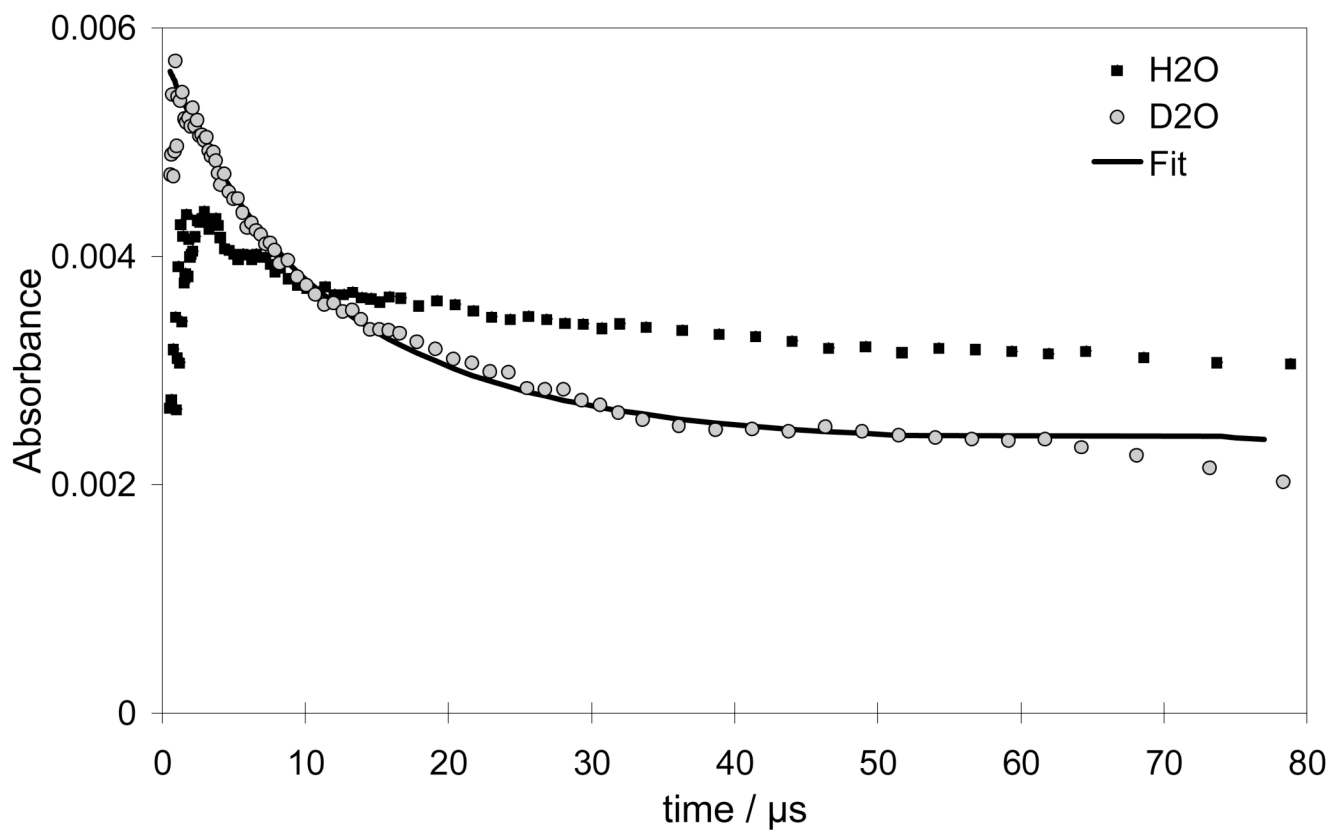
Figure 3.
Pulse radiolysis (20.8 Gy) of 200 μM N-Ac-AlaAlaAspAlaAlaAla, pH 4, N_2O sat. The reaction was followed at 260 nm (circles). The absorption after 50 μs is indicative for K_{14}, in the time range 5 – 30 μs the kinetics are governed by the installation of equilibrium 14 (i.e. $k_{14} + k_{-14}$). To visualize the sensitivity of the simulation on k_{14} results for $k_{14} = 8 \times 10^5$ s^{-1} (too fast, dotted line), $k_{14} = 1 \times 10^5$ s^{-1} (correct value, full line) and $k_{14} = 2 \times 10^4$ s^{-1} (too slow, dashed line) for the given K_{14} are shown.

Figure 4.
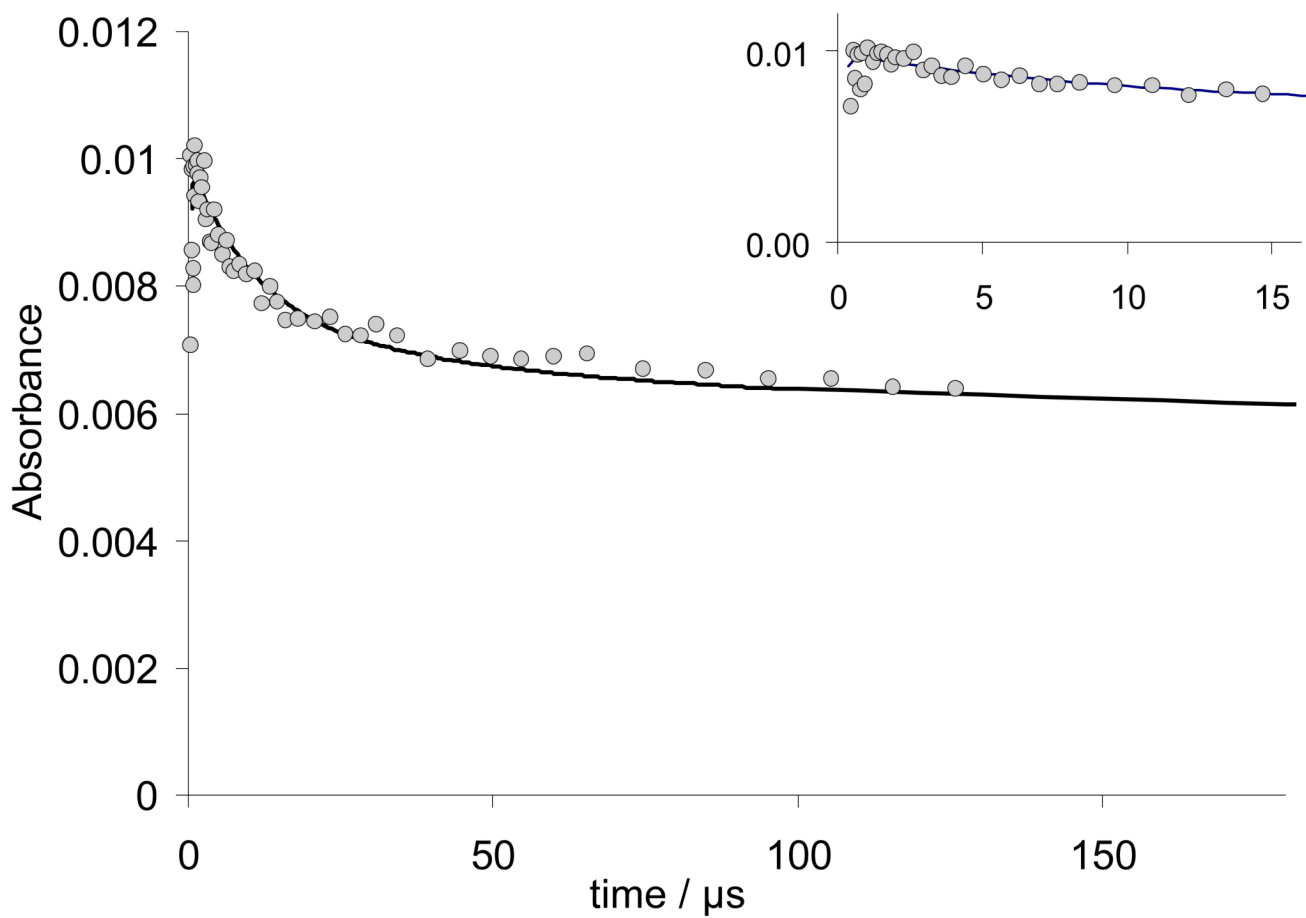Laser flash photolysis (double photon excitation of water, 100 mM at 266 nm with detection at 330 nm) of N_2O sat. solutions of 630 μM N-AcCysGly$_6$ (grey squares in panels A and B) or mixtures of 630 μM N-Ac-Cys and 630 μM N-Ac-Gly-NH$_2$ (grey diamonds in panels A and B). In the former cases, intramolecualr hydrogen transfer (equilibrium 6) is possible, whereas in the latter it is not. The filled circles in panels A and B represent the difference traces, so that the reactions in N-AcCysGly$_6$ are corrected for all second order reactions. These differences represent intramolecular reactions. The kinetic isotope effect between solutions of H_2O (panel A) and D_2O (panel B) are clearly visible. Panel C directly compares the reactions

of N-Ac-CysGly$_6$ in D$_2$O (grey dots, upper trace) with the ones in H$_2$O (black dots, lower trace).
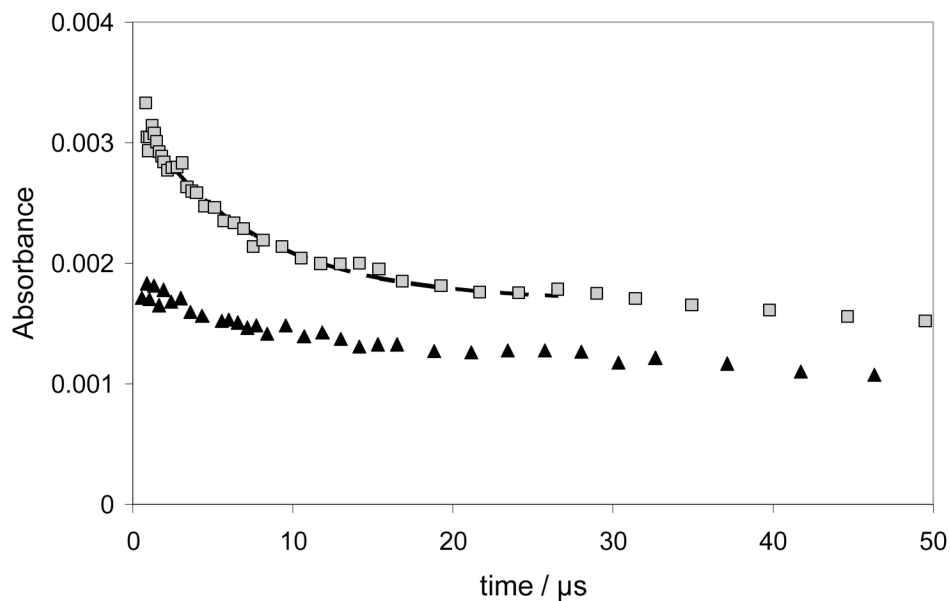
Figure 5.
Identical to figure 4C, but with longer timescale. Instead of a quick installation of an equilibrium in H_2O (black squares, see also figure 4C) we find a much slower one in D_2O. The kinetic isotope effect for the H/D transfer reactions derived from the fit shown here and the data derived from the experiments represented in figures 1, 2 A+B and 4A are $k_{6,H}/k_{6,D} = 6.8$ and $k_{-6,H}/k_{-6,D} = 17.8$. Despite the uncertainty for the latter value we have to assume that there is an influence of tunneling.
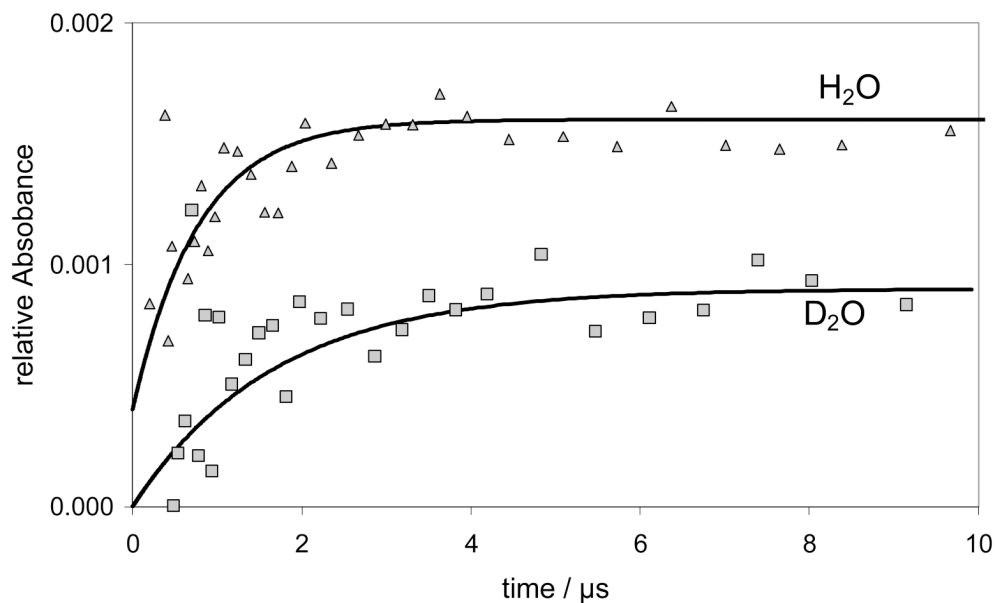
Figure 6.
Laser flash photolysis (double photon excitation of water, 100 mJ at 266 nm with detection at 275 nm) of an N_2O saturated aqueous solution of 613 μM N-Ac-AlaAlaAspAlaAlaAla. All rate constants for the simulation (full line) are taken the same as in figure 3 except for k_{14} which differs by 8% (see table 1)

Figure 7.
Laser flash photolysis of 600 μM 2-mercaptopropioglycine in N_2O saturated water. The excitation wavelength was 266 nm and 100 mJ pulses were used. Grey squares: Reaction in D_2O, black triangles: in H_2O. In D_2O a distinct change of absorption is visible in the time range 3 – 30 μs, which can be described by a first order process with $^{D}k_{obs} = 1.4 \times 10^5$ s-1.

Figure 8.
Laser flash photolysis of $(CysGly)_2$ (disulfide photolysis). The installation of the equilibrium between sulfur and carbon centered radicals is observed. The intramolecular reaction is slower in D_2O, because of isotope effects. The excitation was done with 20 mJ pulses of 266 nm light. The solutions were N_2O saturated and contained 1 mM $(CysGly)_2$. We added 1 M ^tBuOH to scavenge immediately all putative products of double photon photolysis of water. The traces shown are averages of 5 experiments. As the signals are very small, these experiments are considered as proof of concept, because they provide an alternative entry into the radical reaction cascade. Nevertheless, they agree well with the data obtained by pulse radiolysis or double photon photolysis of water.
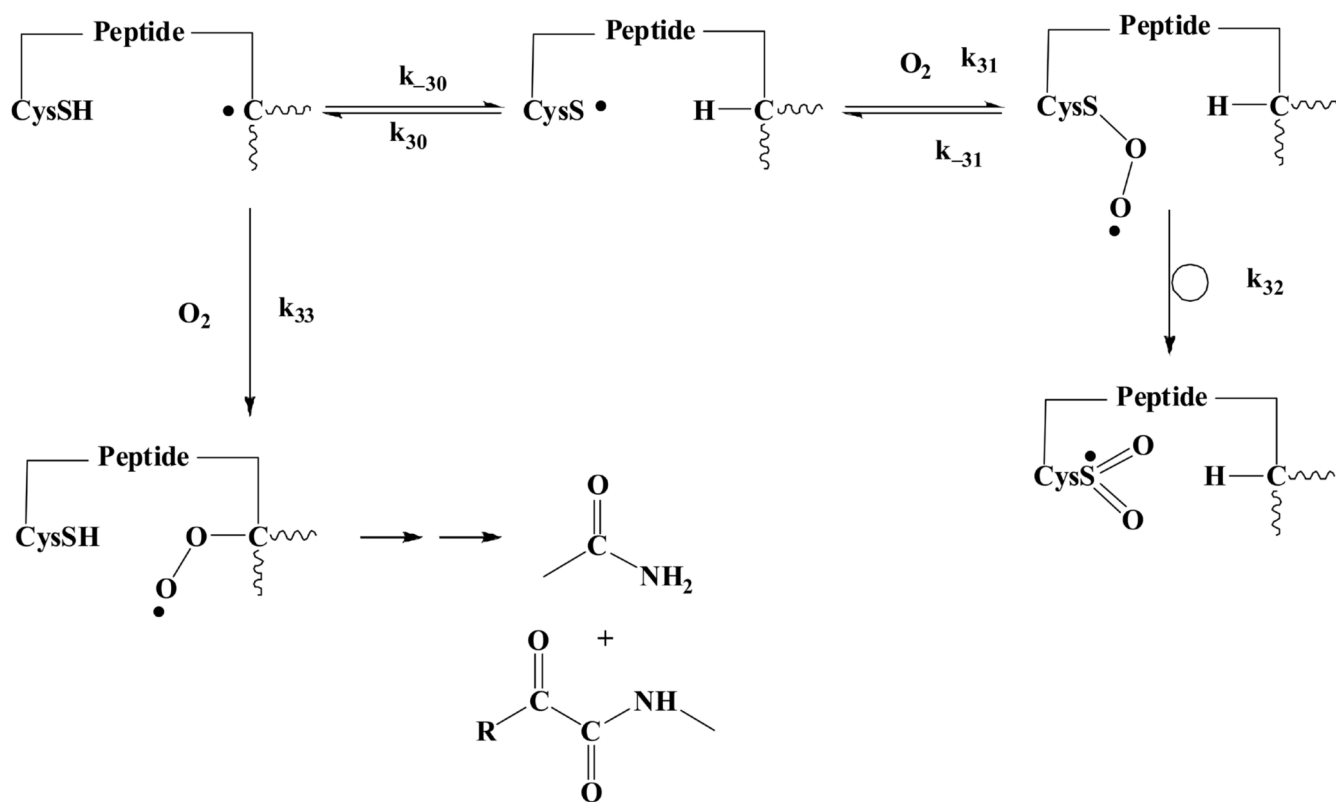
Scheme 1.

Table 1

Rate and equilibrium constants for the reversible hydrogen transfer between Cys thiyl radicals and Gly and Ala in model peptides

Peptide	C-H donor	RS$^\bullet$ + H-C	RSH + $^\bullet$C	K	Method
N-Ac-CysGly$_6$	Gly	$k_6 = (1.1\pm0.1)\times10^5$ s^{-1}	$k_{-6} = (8.9\pm0.4)\times10^5$ s^{-1}	$K_6 = 0.123$	Pulse radiolysis
	Gly	$k_6 = 1.0\times10^5$ s^{-1}	$k_{-6} = 8.9\times10^5$ s^{-1}	$K_6 = 0.123$	LFP
N-Ac-CysGly$_2$AspGly$_3$	Gly	$k_{25} = 1.0\times10^5$ s^{-1}	$k_{-25} = 8.0\times10^5$ s^{-1}	$K_{25} = 0.125$	LFP
N-Ac-CysAla$_2$AspAla$_3$	Ala	$k_{14} = 9.2\times10^3$ s^{-1}	$k_{-14} = 1.0\times10^5$ s^{-1}	$K_{14} = 0.092$	Pulse radiolysis
	Ala	$k_{14} = 1\times10^4$ s^{-1}	$k_{-14} = 1.0\times10^5$ s^{-1}	$K_{14} = 0.100$	LFP